



Pure and silver (2.5–40 vol%) modified TiO₂ thin films deposited by radio frequency magnetron sputtering at room temperature: Surface topography, energy gap and photo-induced hydrophilicity

Fanming Meng^{a,b,c,*}, Fei Lu^{a,c}

^a School of Physics and Materials Science, Anhui University, Hefei 230039, PR China

^b Key Laboratory of Materials Modification by Laser, Ion and Electron Beams (Dalian University of Technology), Ministry of Education, Dalian 116024, PR China

^c Anhui Key Laboratory of Information Materials and Devices, Anhui University, Hefei 230039, PR China

ARTICLE INFO

Article history:

Received 31 January 2010

Received in revised form 31 March 2010

Accepted 2 April 2010

Available online 20 April 2010

Keywords:

Silver

TiO₂ thin film

RF magnetron sputtering

Hydrophilicity

ABSTRACT

Ag–TiO₂ nanostructured thin films with silver volume fraction of 0–40% were deposited on silicon and quartz substrates by radio frequency (RF) magnetron sputtering. The phase structure, surface composition, surface topography, optical properties, and hydrophilicity of the films were characterized by X-ray diffractometer, X-ray photoelectron energy spectrometer, atomic force microscope, ultraviolet–visible spectrophotometer, and water contact angle apparatus. The relation of hydrophilic property and silver content was studied in detail. It was found that silver content influences microstructure of TiO₂ thin films, and silver in the films is metallic Ag (Ag⁰). Hydrophilic behavior of the films increases with the increase of silver content up to 5 vol% Ag and then decreases. A suitable amount (around 5 vol% Ag) of silver addition can significantly enhance the hydrophilicity of TiO₂ films. The hydrophilic behavior of the films is discussed in terms of the synergic effects of defective site, energy gap, surface roughness, and grain size.

© 2010 Elsevier B.V. All rights reserved.

1. Introduction

In 1997, Wang et al. [1] reported that ultraviolet illumination of TiO₂ surfaces could produce a highly hydrophilic surface which was named as super-hydrophilicity. Since then, hydrophilic titanium dioxide materials have been attracting attention for many practical applications such as self-cleaning and antifogging materials. However, the hydrophilic property of the TiO₂ thin films need be further improved and enhanced for practical application. It was reported that the addition of noble metal to a photocatalytic semiconductor can change the semiconductor surface properties [2]. It was also reported that silver nanoparticles show efficient plasmon resonance in the visible region [3]. Although many attentions have been paid to the material doped with noble metals, such as Pt [4], Au [5], and Ag [6], to enhance photocatalytic activity of the TiO₂ thin films; a study on enhance hydrophilic behavior of silver modified TiO₂ thin films has not been reported. Ag–TiO₂ thin films can be prepared by numerous techniques such as thermal oxidation of electron-beam-evaporated [7], SILAR method [8], sol–gel

processes [9], pulsed laser deposition method [10], and sputtering [11]. Among these techniques, RF magnetron sputtering method provides more advantages, such as a small quantity of adventitious impurity, small stress, excellent uniformity property, etc., in controlling the microstructure and composition of the films. In this paper, Ag–TiO₂ nanostructured thin films were deposited on silicon and quartz substrates by RF magnetron sputtering at room temperature. Our main purpose is to investigate the influence of silver content on crystal structure, surface topography, energy gap, and photo-induced hydrophilicity of the films.

2. Experimental details

2.1. Preparation of samples

Ag–TiO₂ nanostructured thin films with various silver content (0–40 vol%) were prepared by a JGP560I-type high vacuum multifunctional magnetron sputtering equipment, made by Scientific Instrument Development Center Limited Company of China, using Ag–TiO₂ ceramic targets ($\Phi = 60$ mm) on silicon (10 mm \times 10 mm) and quartz (25.1 mm \times 15.4 mm) substrates at room temperature. The targets were made by sticking Ag strips (99.99% purity) onto TiO₂ target (99.99% purity). Prior to deposition, the substrates were ultrasonically cleaned with acetone, absolute ethyl alcohol, and de-ionized water for 10 min, respectively. When the sputtering chamber was evacuated to a base pressure of 8×10^{-4} Pa, argon gas (99.99% purity) was introduced. Before the films were deposited, Ag–TiO₂ ceramic target was pre-sputtered by argon ion for 3 min to weed out the surface adsorption. During sputtering, argon gas flow rate was kept at 30 sccm, the chamber pressure was maintained at 0.8 Pa, the sputtering power was 60 W, and the distance between the

* Corresponding author at: School of Physics and Materials Science, Anhui University, 3 Feixi Road, Hefei 230039, Anhui Province, PR China. Tel.: +86 551 5107284; fax: +86 551 5107237.

E-mail addresses: mrmeng@ahu.edu.cn, mrmeng@tom.com (F. Meng).

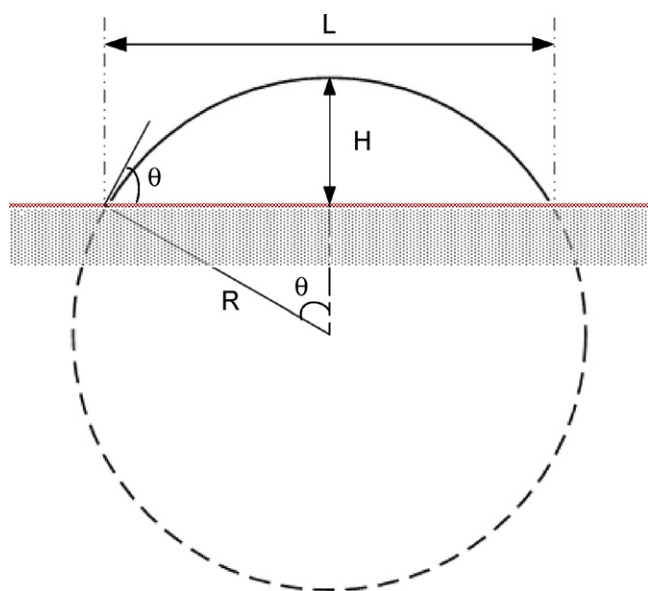


Fig. 1. Geometric pattern for calculation of water contact angle [12].

substrate and the target was 60 mm. In order to obtain the same film thickness, sputtering time was 27, 25.3, 24, 22, 18, and 11.7 min corresponding with silver content of 0, 2.5, 5, 10, 20, and 40 vol%, respectively, due to their different sputtering rate.

2.2. Characterization

The thickness of the films corresponding with silver content of 0, 2.5, 5, 10, 20, and 40 vol%, measured by a surface profiler meter (Ambios XP-1), is 112, 116, 122, 109, 112, and 123 nm, respectively. The error of the measurements was ± 0.1 nm. The crystallization behavior of the films was analyzed by a MAC M18XHF X-ray diffractometer, made by MAC Science Limited Company of Japan, using Cu K α radiation. The accelerating voltage is 40 kV, current 100 mA, scanning range 20–80°, scanning step 0.02°, and scanning speed 8°/min. The surface composition was analyzed by an ESCALAB 250 X-ray photoelectron energy spectrometer, made by Thermo Electron Company of America. The working pressure in the XPS chamber was approximately 10^{-6} Pa. Al K α radiation was obtained by an accelerating voltage of 15 kV and an emission current of 12 mA. Survey spectra were collected with a scanning step of 1 eV. All the binding energies were referenced to the C1s peak at 284.8 eV of the surface adventitious carbon. Surface morphological features were observed by an AJ-IIIa-type atomic force microscope made by Shanghai AJ Nano-Science Development Limited Company of China. The AFM operating mode is tap. Transmission spectra were obtained by an ultraviolet–visible spectrophotometer (SHIMADZU UV-2550(PC) SERIES). The energy gap was determined by plotting $(\alpha h\nu)^{1/2}$ versus equivalent energy at the wavelength λ .

2.3. Hydrophilicity measurements

The photo-induced hydrophilic property of the films was evaluated by screening photos and measuring the contact angle of water droplet during irradiation of a 36W high pressure mercury lamp, which emits visible light of 404.7, 435.8, 546.1 and 577.0–579.0 nm, and ultraviolet light of 365 nm. The hydrophilicity photos were obtained by a home-made water contact angle apparatus, which was performed at ambient air (25 °C, relative humidity (RH) 60%). By measuring the diameter and height of the spherical crown of 3 mL droplet dropped on the surface of the films from 2 mm height, the water contact angle can be calculated from Eq. (1):

$$\theta = \arctan \frac{4HL}{L^2 - 4H^2} \quad (1)$$

where θ is water contact angle, L is diameter of the spherical crown, H is height of the spherical crown, as shown [12] in Fig. 1.

3. Results and analysis

3.1. X-ray diffraction (XRD) analysis

Fig. 2 shows XRD patterns of (a) pure and (b) 2.5, (c) 5, (d) 10, (e) 20, and (f) 40 vol% Ag modified TiO₂ thin films on silicon substrates. We can see that phase structure of the films changes with the increase of silver content. The pure TiO₂ thin films possess

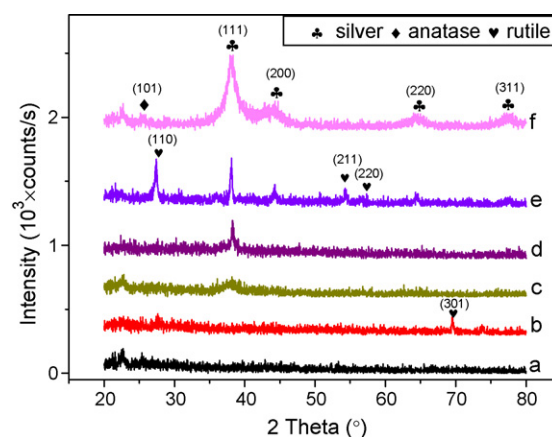


Fig. 2. XRD patterns of (a) pure and (b) 2.5, (c) 5, (d) 10, (e) 20, and (f) 40 vol% Ag modified TiO₂ thin films as deposited on silicon substrate.

irregular background noise and no characteristic peaks of brookite, anatase, rutile, and silver at all, suggesting that the film is amorphous. When silver content is 2.5 vol%, there are slightly diffraction peaks of 27.70 and 69.58°, which are corresponding to rutile (1 1 0) and (3 0 1), respectively. When silver content increases to 5 vol%, the diffraction peak of silver (1 1 1) appears, and then with further increase of silver content, the peak intensity gradually increases. In the XRD pattern of 20 vol% Ag modified TiO₂ thin film, there are diffraction angles of 27.70, 38.05, 44.34, 54.37, 56.71, 64.58, and 77.42°, which are corresponding to rutile (1 1 0), silver (1 1 1), silver (2 0 0), rutile (2 1 1), rutile (2 2 0), silver (2 2 0), and silver (3 1 1), respectively. In the XRD pattern of 40 vol% Ag modified TiO₂ thin film, there are diffraction angles of 25.36, 38.05, 44.34, 64.58, and 77.42°, which are corresponding to anatase (1 0 1), silver (1 1 1), silver (2 0 0), silver (2 2 0), and silver (3 1 1), respectively. All these analysis suggest that silver content influences phase structure of Ag–TiO₂ thin films, and silver in the films is metallic Ag (Ag⁰).

3.2. X-ray photoelectron spectroscopy (XPS) analysis

Fig. 3 shows the XPS survey spectrum for the surface of 10 vol% Ag modified TiO₂ thin films as deposited. The result illustrates that silver, titanium, oxygen and carbon are found in the 10 vol% Ag modified TiO₂ thin films. The atomic concentration of these elements were calculated and listed in Table 1.

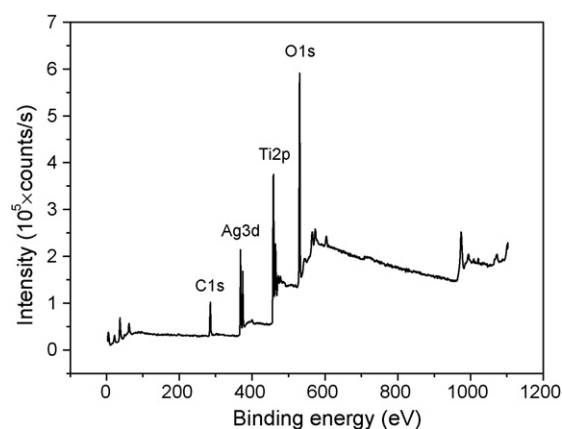


Fig. 3. XPS survey spectrum for the surface of 10 vol% Ag modified TiO₂ thin films as deposited.

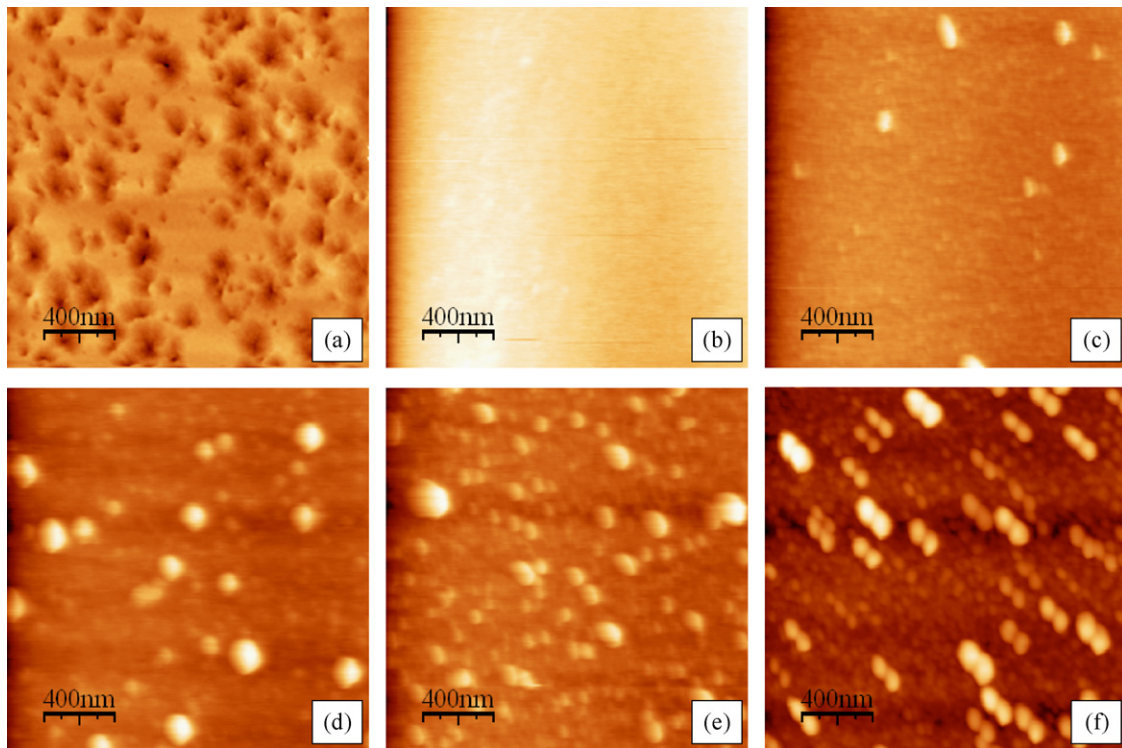


Fig. 4. AFM images of (a) pure and (b) 2.5, (c) 5, (d) 10, (e) 20, and (f) 40 vol% Ag modified TiO₂ thin films as deposited on silicon substrate.

3.3. Atomic force microscope (AFM) analysis

Fig. 4 shows AFM images of (a) pure and (b) 2.5, (c) 5, (d) 10, (e) 20, and (f) 40 vol% Ag modified TiO₂ thin films on the silicon substrate. Fig. 5 depicts influence of silver content on grain size and surface roughness of the films, as deduced from AFM measurements. From Figs. 4 and 5, we can see that there is not any particle on the surface of pure TiO₂ film, but silver modified TiO₂ thin films are all composed of mono-dispersed sphere-like particles. With the increase of silver content from 0 to 40 vol%, grain size and surface roughness of the films decrease first and then increase and quantity of particles increase evidently. Obviously, surface roughness is rather well correlated to the grain size, which suggests that roughness of the films is at least partially induced by grain size effects.

3.4. Ultraviolet–visible (UV–vis) spectrometer analysis

Fig. 6 shows transmission spectra of the films on quartz substrates. We can see that absorption edges for silver modified TiO₂ thin films shift to longer first and then shorter wavelength. The transmission spectra of all samples show a sharp decrease in the UV region due to fundamental absorption of light. In the visible region, the light-scattering dominates over the absorption, and the light-scattering losses increase with increasing grain size, however, at wavelengths close to the absorption edge, the light-scattering losses are dominated by the fundamental absorption [13,14]. Optical transmittance spectrum can be used to derive the energy gap

Table 1
Atomic concentration of different elements in 10.0 vol% Ag modified TiO₂ thin films as deposited determined by XPS.

	Elements			
	Ag	Ti	O	C
Atomic concentration (%)	3.7	20.93	53.53	21.84

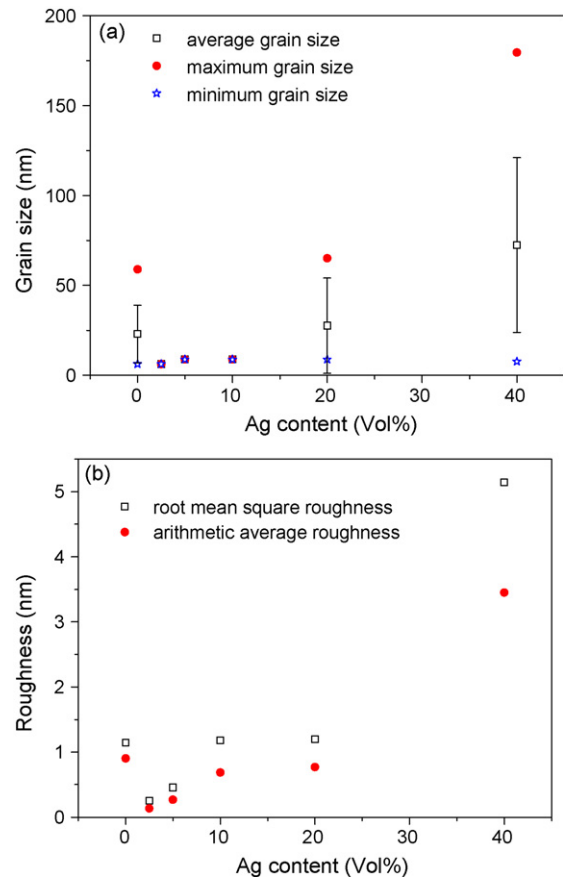


Fig. 5. Influence of silver content on (a) grain size and (b) surface roughness of Ag–TiO₂ thin films as deposited on silicon substrate. (Note: standard error on average grain size measurements is 16.028, 0.000, 0.000, 0.000, 26.523, and 48.630 nm, for pure and 2.5, 5, 10, 20, and 40 vol% Ag modified TiO₂ thin films, respectively.)

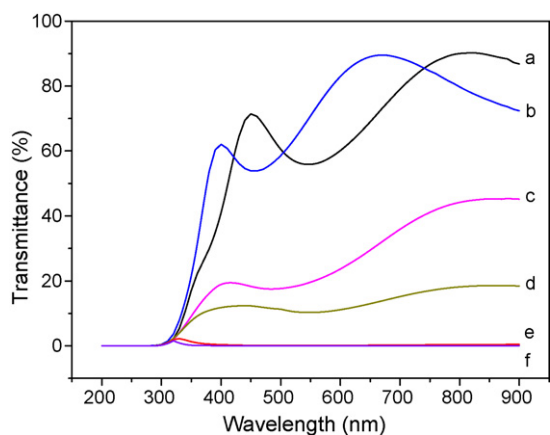


Fig. 6. Transmission spectra of (a) pure and (b) 2.5, (c) 5, (d) 10, (e) 20, and (f) 40 vol% Ag modified TiO₂ thin films as deposited on quartz substrate.

(E_g) of the films, which is determined [15,16] by plotting $(\alpha h\nu)^{1/2}$ versus equivalent energy at the wavelength λ , as a result, the energy gap is 3.02, 3.00, 2.81, 2.87, 2.92, and 2.97 eV, for (a) pure and (b) 2.5, (c) 5, (d) 10, (e) 20, and (f) 40 vol% Ag modified TiO₂ thin films, respectively. We can see that the energy gap of silver modified TiO₂ thin films decreases with the increase of silver content up to 5 vol% Ag and then increases.

3.5. Hydrophilicity

Fig. 7 shows water contact angles of (a) pure and (b) 2.5, (c) 5, (d) 10, (e) 20, and (f) 40 vol% Ag modified TiO₂ thin films on quartz substrates as a function of irradiation time of high pressure mercury lamp. We can see that water contact angles of the films decreases with the increase of silver content up to 5 vol% Ag and then increases. For the same sample, the water contact angle decrease with the increase of irradiation time, which means the surface converts to hydrophilic state. And it seems that for the 5 vol% Ag modified film, the high hydrophilicity could be achieved easily.

3.6. The mechanism of hydrophilicity

From the above results we can see that irradiation of pressure mercury lamp can induce hydrophilicity of TiO₂ thin films. This is called photo-induced hydrophilicity, which shown in the

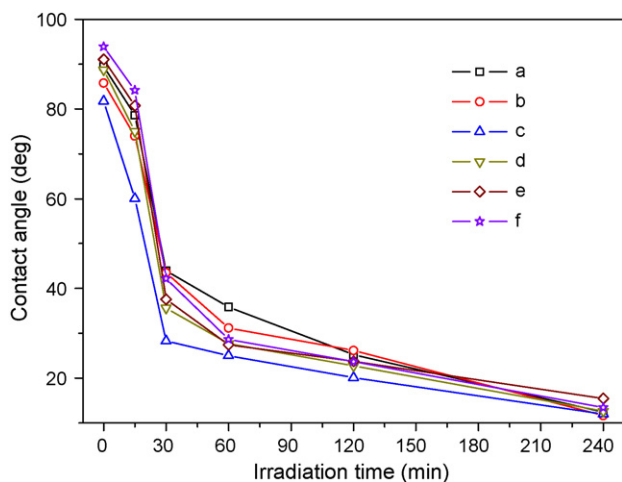


Fig. 7. Water contact angles of (a) pure and (b) 2.5, (c) 5, (d) 10, (e) 20, and (f) 40 vol% Ag modified TiO₂ thin films as deposited on quartz substrate as a function of irradiation time of high pressure mercury lamp.

change of the water contact angle with irradiation time. The mechanism of photo-induced hydrophilic behavior of TiO₂ thin films has been intensively investigated by many researchers [17–19]. It was revealed that preferential adsorption of water molecules on the photo-generated surface defective sites led to the formation of highly hydrophilic TiO₂ thin films surface [19,20]. Photo-generated electron–hole pairs could either recombine or move to the surface to react with species adsorbed on the surface. Some of the electrons react with lattice metal ions Ti⁴⁺ to form Ti³⁺ defective sites [21]. The formation processes of defective sites on TiO₂ surface can be expressed as follows [22]:



In air, the surface trapped electrons (Ti³⁺) tend to react immediately with O₂ adsorbed on the surface to form O₂⁻ or O₂²⁻ ions. Meanwhile, water molecules may coordinate into the oxygen vacancy sites (V_O), which leads to dissociative adsorption of the water molecules on the surface [22–24]. This process gives rise to the increase of hydroxyl content on the illuminated TiO₂ thin film surfaces. It was likely that the number of defective sites increased with the increase of silver content and this led to the improvement of hydrophilicity. From Section 3.5 it can be seen that water contact angles of the films decreases with the increase of silver content up to 5 vol% Ag and then increases which means that the amount of defective sites increases with the increase of silver content up to 5 vol% Ag and then decreases. And we can also see that with the increase of silver content from 0 to 40 vol%, the water contact angle and energy gap show the same change rule, namely the lower the energy gap is, the smaller the water contact angle is. The reason is that the film with lower energy gap has more photo-generated electrons contributed from the valence band and the conduction band [25]. The more electrons that are excited, the more reactive the surface is to water on the thin film. Here, the energy gap are 3.02, 3.00, 2.81, 2.87, 2.92, and 2.97 eV, for (a) pure and (b) 2.5, (c) 5, (d) 10, (e) 20, and (f) 40 vol% Ag modified TiO₂ thin films, respectively. We can calculate that threshold absorption wavelength are 411.6, 414.4, 442.4, 433.1, 425.7, and 418.6 nm, for (a) pure and (b) 2.5, (c) 5, (d) 10, (e) 20, and (f) 40 vol% Ag modified TiO₂ thin films, respectively. Owing to the high pressure mercury lamp emits visible light of 404.7, 435.8, 546.1, and 577.0–579.0 nm, and ultraviolet light of 365 nm; so we can know that all the films can absorb the ultraviolet light of 365 nm and visible light of 404.7 nm from irradiation of high pressure mercury lamp, but as a exception, 5 vol% Ag modified TiO₂ thin films can also absorbs visible light of 435.8 nm. The 5 vol% Ag modified TiO₂ thin films has a lower energy gap, produces more excited electrons, and exhibits higher photo-induced hydrophilicity.

In addition, it was reported [26] that the photo-induced hydrophilic conversion of film surface is directly correlated with surface morphology. For a better understanding of surface topography effects on the photo-induced hydrophilic conversion on the silver modified TiO₂ thin films, the relationships between the contact angle and surface roughness and grain size were analyzed. From Figs. 5 and 7, we can see that contact angle and surface roughness together with grain size show approximately the same change rule with the increase of silver content, which reveals that hydrophilic behavior of the films surface is directly correlated with surface roughness and grain size. As reported in literatures [27–29], the small grain size lead to higher hydrophilicity of TiO₂ surface, a fact was observed here.

Based on above discussion, it was suggested that the extension of visible light absorption region and the increase of defective sites are main causes of enhanced hydrophilicity for silver modified TiO₂ films. In addition, the hydrophilic property of the films surface is directly correlated with surface roughness and grain size.

4. Conclusions

In conclusion, water contact angle of the films decreases with the increase of silver content up to 5 vol% Ag and then increases. For the same sample, the water contact angle decrease with increase of irradiation time, and it seems that for the 5 vol% Ag modified film, the high hydrophilicity could be achieved easily. Silver content influences phase structure of TiO₂ thin films, and silver in the films is metallic Ag (Ag⁰). With the increase of silver content from 0 to 40 vol%, grain size and surface roughness of the films decrease first and then increase and quantity of particles increase evidently, and the energy gap decreases first and then increases. The extension of visible light absorption region and the increase of defective sites are main causes of enhanced hydrophilicity for the films, and the hydrophilicity of the films surface is directly correlated with surface roughness and grain size.

Acknowledgements

This work was supported by the National Natural Science Foundation of China (No. 50872001), the Scientific Research Foundation of Education Ministry of Anhui Province of China (Nos. KJ2009A006Z and KJ2007B132), the Doctor Scientific Research Starting Foundation of Anhui University of China, and the Foundation of Construction of Quality Project of Anhui University of China (No. XJ200907).

References

- [1] R. Wang, K. Hashimoto, A. Fujishima, M. Chikuni, E. Kojima, A. Kitamura, M. Shimohigoshi, T. Watanabe, *Nature* 388 (1997) 431.
- [2] A.L. Linsebigler, G.Q. Lu, J.T. Yates Jr., *Chem. Rev.* 95 (1995) 735.
- [3] P. Wang, B.B. Huang, X.Y. Qin, X.Y. Zhang, Y. Dai, J.Y. Wei, M.-H. Whangbo, *Angew. Chem. Int. Ed.* 47 (2008) 7931.
- [4] A.Z. Simões, F.G. Garcia, C.S. Riccardi, *J. Alloys Compd.* 493 (2010) 158.
- [5] Z.Y. Chen, Y. Hu, T.C. Liu, C.L. Huang, T.S. Jeng, *Thin Solid Films* 517 (2009) 4998.
- [6] K. Nakata, K. Udagawa, D.A. Tryk, T. Ochiai, S. Nishimoto, H. Sakai, T. Murakami, M. Abe, A. Fujishima, *Mater. Lett.* 63 (2009) 1628.
- [7] Y.Y. Zhang, X.Y. Ma, P.L. Chen, D.R. Yang, *J. Alloys Compd.* 480 (2009) 938.
- [8] U.M. Patil, K.V. Gurav, O.S. Joo, C.D. Lokhande, *J. Alloys Compd.* 478 (2009) 711.
- [9] M.C. Wang, H.J. Lin, T.S. Yang, *J. Alloys Compd.* 473 (2009) 394.
- [10] G. Shukla, P.K. Mishra, A. Khare, *J. Alloys Compd.* 489 (2010) 246.
- [11] Y.Y. Liu, L.Q. Qian, C. Guo, X. Jia, J.W. Wang, W.H. Tang, *J. Alloys Compd.* 479 (2009) 532.
- [12] F.M. Meng, L. Xiao, Z.Q. Sun, *J. Alloys Compd.* 485 (2009) 848.
- [13] S. Schiller, G. Beister, W. Sieber, *Thin Solid Films* 83 (1981) 239.
- [14] D. Mardare, D. Luca, C.M. Teodorescu, D. Macovei, *Surf. Sci.* 601 (2007) 4515.
- [15] D. Mardare, G.I. Rusu, F. Iacomi, M. Girtan, I. Vida-Simiti, *Mater. Sci. Eng. B* 118 (2005) 187.
- [16] D. Mardare, F. Iacomi, D. Luca, *Thin Solid Films* 515 (2007) 6474.
- [17] R. Wang, K. Hashimoto, A. Fujishima, M. Chikuni, E. Kojima, A. Kitamura, M. Shimohigoshi, T. Watanabe, *Adv. Mater.* 10 (1998) 135.
- [18] R. Sun, A. Nakajima, N. Sakai, A. Fujishima, T. Watanabe, K. Hashimoto, *J. Phys. Chem. B* 105 (2001) 1984.
- [19] J.C. Yu, J. Yu, W. Ho, J. Zhao, *J. Photochem. Photobiol. A: Chem.* 148 (2002) 331.
- [20] M.R. Hoffman, S.T. Martin, W. Choi, D.W. Bhamann, *Chem. Rev.* 95 (1995) 69.
- [21] S.D. Sharma, D. Singh, K.K. Saini, C. Kant, V. Sharma, S.C. Jain, C.P. Sharma, *Appl. Catal. A: Gen.* 314 (2006) 40.
- [22] N. Sakai, A. Fujishima, T. Watanabe, K. Hashimoto, *J. Phys. Chem. B* 105 (2001) 3023.
- [23] R. Wang, N. Sakai, A. Fujishima, T. Watanabe, K. Hashimoto, *J. Phys. Chem. B* 103 (1999) 2188.
- [24] N. Sakai, R. Wang, A. Fujishima, T. Watanabe, K. Hashimoto, *Langmuir* 14 (1998) 5918.
- [25] H.Y. Chou, E.K. Lee, J.W. You, S.S. Yu, *Thin Solid Films* 516 (2007) 189.
- [26] M. Sucheas, S. Christoulakis, I.V. Tudose, D. Vernardou, M.I. Lygeraki, S.H. Anastasiadis, T. Kitsopoulos, G. Kiriakidis, *Mater. Sci. Eng. B* 144 (2007) 54.
- [27] M. Anpo, T. Shima, S. Kodama, Y. Kubokawa, *J. Phys. Chem.* 91 (1987) 4305.
- [28] T.M. Wang, S.K. Zheng, W.C. Hao, C. Wang, *Surf. Coat. Technol.* 155 (2002) 141.
- [29] X. Jiang, X.M. Chen, *J. Cryst. Growth* 270 (2004) 547.